IEEE Access
Multidisciplinary ⋮ Rapid Review ⋮ Open Access Journal

Received November 8, 2019, accepted November 26, 2019, date of publication December 2, 2019,
date of current version December 23, 2019.

Digital Object Identifier 10.1109/ACCESS.2019.2956982

Piecewise Nonlinear Dynamic Modeling for Gear Transmissions With Rotary Inertia and Backlash

ZHEN XU[1,2,3], HUA DENG[1,2], (Member, IEEE), AND YI ZHANG[1,2]
[1]School of Mechanical and Electrical Engineering, Central South University, Changsha 410083, China
[2]State Key Laboratory of High Performance and Complex Manufacturing, Changsha 410083, China
[3]China Railway Construction Heavy Industry Company, Ltd., Changsha 410100, China

Corresponding author: Yi Zhang (zhangyicsu@csu.edu.cn)

This work was supported by the National Basic Research Program of China under Grant 2006CB705404.

ABSTRACT Establishing an accurate dynamic model for gear transmission is challenging because of the complex dynamic mechanical behavior of the gear transmission, particularly under difficult working conditions such as heavy loads and frequent starts and stops. This feature significantly increases the difficulty level of the dynamic analysis, control, and real-time fault diagnosis of such a gear transmission, given that sufficiently accurate dynamic models are indispensable for them. Thus, this study proposes a piecewise nonlinear model for gear transmissions by considering rotary inertia, backlash, and friction in control applications under difficult working conditions. The model parameters of gear transmissions can be calculated by using analytical calculation formulas. The experiments are conducted for the gear transmission system of a heavy-duty manipulator in start–stop and continuous rotation conditions. The experimental results show that the proposed piecewise nonlinear model is in good agreement with the practical dynamic gear transmission behavior, which is feasible for the control applications of gear transmissions under difficult working conditions.

INDEX TERMS Dynamic modeling, gear transmission, piecewise nonlinear model, rotary inertia, backlash.

I. INTRODUCTION

Gear transmission is an indispensable part of many common mechanical systems, such as robotic manipulators, vehicles, and aerospace [1]–[4]. It is an extremely complicated process that involves multibody engagement and multipoint contact [5], particularly under heavy load conditions with frequent starts and stops, such as the conditions used in forging manipulators [6], excavators [7], and palletizing robots [8]. An example of typical dynamic systems is the gear transmission system of a heavy-duty forging manipulator [6], which is widely used in the forging industry [9]. The forging manipulator often cooperates with a forging press to form forge pieces under heavy load and low speed, wherein the output torque of the gear transmission system may reach up to 1200 kN·m. In the forging process, the forge pieces that are gripped by a gripper with two tong arms should be turned, thereby requiring the gear transmission system to start and stop frequently. An impact-like torque exists in this process [6]. Frequent starts and stops and the existence of backlash allow gear transmission systems to produce intermittent motion, which greatly affects the gear. In this case, the dynamic characteristics of the gear transmission system differ from those that operate at a specified speed [1], [10], [11]. In addition, the effect of sliding friction on the dynamics of the gear pair, particularly under heavy loads, may not be neglected [12]–[16]. Establishing accurate dynamic models is challenging because the working conditions of such gear transmission systems are extremely difficult. This feature significantly increases the difficulty level of the dynamic analysis, control, and real-time fault diagnosis of such gear transmissions, given that sufficiently accurate dynamic models are indispensable for them [1], [17].

Researchers have reported investigations on gear transmission dynamics given that gears usually transmit rotary motion and power through the interaction force between gear teeth [18], [19]. In particular, the finite-element/contact mechanical formulation was used to accurately capture the nonlinear dynamics of the gear pairs [20], [21]. However, the practical application can hardly be realized given the high computational cost and lack of tools for the cosimulation of finite elements and multibody dynamic modeling. Therefore, Ziegler and Eberhard [11] presented a modally reduced elastic multibody model with collision detection that could

The associate editor coordinating the review of this manuscript and approving it for publication was Porfirio Tramontana.

describe the important elastic effects for overcoming the high computational cost. The results obtained using this approach are consistent with those of the corresponding finite-element analysis. Nevertheless, the model cannot be applied in practical control systems because a sufficiently accurate analytic model is needed. A multitooth contact dynamic model for gear meshing was presented to simulate the discontinuous meshing in gear transmission [22]. However, the derivation of the model lacks a relevant theoretical basis and an experimental verification. Although numerous studies on establishing analytic dynamic models for gear transmissions are available [5], [23]–[26], they all focus on the design, vibration, and noise control of gear transmission systems and are usually run under stationary working conditions (e.g., running at a certain working speed). Moreover, few studies have considered backlash and sliding friction, which considerably affect the dynamics of gear transmission systems under nonstationary working conditions, particularly for heavy loads and frequent start-stop operations.

Generally, the meshing contact of gear teeth in a forging manipulator can be regarded as the power source of a robotic end effector to drive the rotation motion of the tong arms. Thus, the contact model of robotic manipulators can be introduced to construct the analytic dynamic model of gear transmission systems. The contact modeling and simulation of robotic dynamics has progressed significantly in the past two decades. Several approaches for capturing the contact dynamics associated with certain tasks in the context of general multibody simulations are available. Robotic contact models can be characterized on the basis of two different approaches [27]. The first approach is suggested by Weber *et al.* [28]. This approach uses a restitution coefficient, which describes the variations of certain dynamic or kinematic parameters, such as the relative velocities caused by the impact between two or more bodies. The second approach is the use of the Kelvin-Voigt [29] (linear) model, which is further extended in [30]; or the Hunt-Crossley [31], [32] (nonlinear) model, which has been developed to continuously describe the relationship between the penetration of the body and the consequent reaction force. These models can be applied to describe the contact dynamics between the end effector of a robotic manipulator and the surrounding objects. These models are suitable when the environment tends to be stationary or quasi-static [33]. However, they are not suitable for the considered gear transmission systems because of their complex behavior under heavy load and frequent start-stop conditions. Zhang and Sharf [34] established an impact experimental setup, which constituted a dynamic system under impact and constructed a dynamic model of the experimental impact to investigate the dynamic contact/impact problem of the bodies. The experimental result indicates that the Hunt-Crossley model does not properly demonstrate the viscoelastic energy dissipation mechanism that occurs in rigid-body impacts. These analyses suggest a new piecewise nonlinear interaction force model based on the Hunt-Crossley model [31], [32] and the result in Zhang and Sharf [34], which considers rotary inertia, backlash, and friction with heavy loads and the start and stop motion proposed for the gear transmission systems. It is different from the existing dynamic models of gear transmission under stationary working conditions [5], [23]–[26]. Due to the impact state of two rigid bodies in collision extended from one rigid body impacting another fixed rigid body [34] to one rigid body impacting another unfixed rigid body, the dynamic transmission characteristics of the latter under the impact force are more in line with the practical dynamic behavior in heavy-duty gear transmission with frequent starts and stops. Experiments of gear transmission for a heavy-duty forging manipulator [6] under frequent start-stop and stationary working conditions demonstrate that the proposed piecewise nonlinear model can better describe the dynamic characteristics of gear transmission under different working conditions.

This work is organized as follows. Sect. II introduces the preliminary information on gear transmission and interaction force. Sect. III proposes a piecewise nonlinear interaction force model of gear transmission with rotary inertia, backlash, friction, and contact ratio. Sect. IV discusses the experiments on gear transmission. Finally, Sect. V provides the conclusions.

II. PRELIMINARY

A. GEAR MESHING PRINCIPLE

Fig. 1 shows a pair of involute spur gears meshing. The gear wheels rotate around centers O_1 and O_2. Line I_1I_2 refers to the common tangent to the two base circles, which generate the involute profiles. P is the pitch point, and r_1 and r_2 are the radii of the basic circles for the pair of spur gears. The teeth are in contact at point O, which is the origin of our coordinate frame of reference. The z-axis is the common normal to the two teeth through O coinciding with I_1I_2. The x-axis lies in the tangent plane, which is in the plane of rotation.

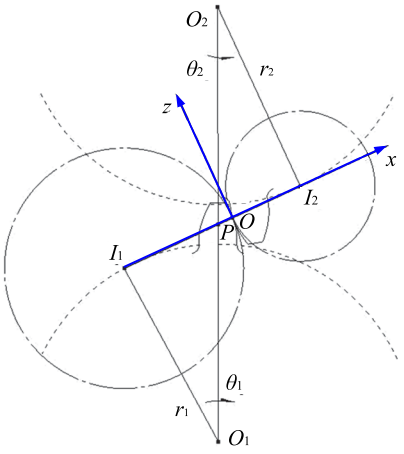

FIGURE 1. Schematic of involute spur gear transmission.

The rolling and sliding motions at a given instant in the meshing cycle can be described by two circles of radii I_1O and I_2O that rotate with angular displacements θ_1 and θ_2 around

fixed centers I_1 and I_2, respectively. Given that the meshing contact of the spur gear transmission exists entirely in the x-z plane, the contact force considered in this paper can be regarded as a point contact force. The contact force under a given external load can be similarly analyzed using the radii of the curvatures of the involute gear teeth at O, which are the same as I_1O and I_2O.

In the dynamic modeling of the gear transmission, the gear meshing is achieved by the interaction force between the gear teeth, which is distributed on different meshing teeth between the pinion and the gear. Fig. 2 illustrates that the interaction force of each meshing point can be decomposed into its normal and tangential components along the z-axis and x-axis, respectively,

$$\vec{F}_c = \vec{F}_n + \vec{F}_t \tag{1}$$

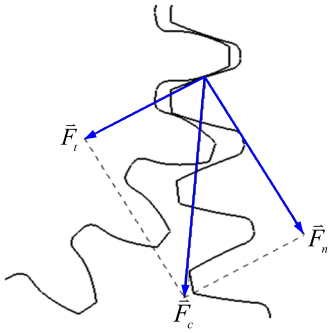

FIGURE 2. Interaction force model between the gear teeth.

where $\vec{F}_n$ is the vector of the normal force along the z-axis, and $\vec{F}_t$ is the vector of the tangential force along the x-axis, $\vec{F}_c$ is the vector sum of the normal force $\vec{F}_n$ and the tangential force $\vec{F}_t$.

B. NONLINEAR INTERACTION FORCE MODEL WITH MASS OF IMPACTED BODY

The spring-dashpot model is a normal contact force model that is popularly used to define the normal force component of the robotic manipulator [27]:

$$F_n(t) = \begin{cases} k\delta(t) + b\dot{\delta}(t) & \delta \geq 0 \\ 0 & \delta < 0 \end{cases} \tag{2}$$

where the coefficients of meshing stiffness k and hysteretic damping b are related to the local indentation $\delta(t)$, which is simplified as δ, and its rate to the normal force at each contact point. The local indentation δ at each contact point can be calculated according to the geometry and location of the two mating surfaces.

When the indentation is small, the contact force depends mainly on the damping term, which is assumed to be independent on the local indentation δ in Eq. (2). Therefore, the spring-dashpot model is linear. Hunt and Crossley [31] [32] proposed a contact force model that defines the normal contact force with a nonlinear relationship of the indentation $\delta(t)$

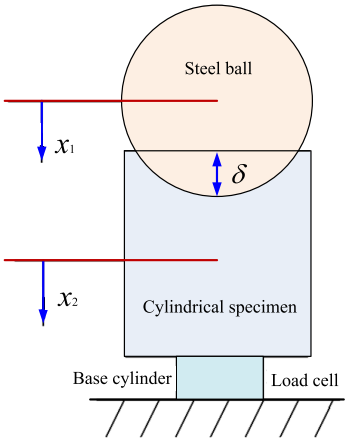

FIGURE 3. Impact experimental platform.

as follows:

$$F_n = \begin{cases} k\delta^{\lambda} + b\delta^{\lambda}\dot{\delta} & \delta \geq 0 \\ 0 & \delta < 0 \end{cases} \tag{3}$$

where $\lambda(1 \leq \lambda \leq 2)$ is a power exponent that is usually close to one. Considering that the contact surface is related to the penetration depth, the exponent λ is affected by the stiffness variation due to the large contact area. Table 1 shows that $\lambda = 1.5$ according to Hertzian theory [35]. A significant improvement in Eq. (3) is its prediction of the zero-impact force at the beginning point and end point of contact and the consistency with the actual physical objects [31]. However, given that the gear transmission for the forging manipulator works under heavy load and low speed conditions, the local indentation δ of gear teeth is larger than the general gear transmission with light load in the contact position. Moreover, these two models only represent the contact relationship between the robot and its contact environment, which is assumed to be stationary or quasi-static [33]. Gear transmission is a dynamic meshing process, and the gear backlash also exists because of the actual manufacturing and assembling errors. Notably, these influencing factors are not considered in Eqs. (2) and (3).

Zhang and Sharf [34] established an impact experimental platform that is composed of a steel ball, a cylindrical specimen, a load cell, and a base cylinder to further study the contact/impact problem (Fig. 3). The Hunt-Crossley model [31] [32] was used and combined with Newton's second law to establish a dynamic test bed model. The experiment assumes that a ball impacts a fixed surface. However, the impacted surface or body is not generally fixed in the real world but is basically in a motion state. Therefore, the model can be derived by multiplying the mass coefficient $\gamma = m_2/m_1$ (where $m_1 \neq 0$) as follows:

$$m_2\ddot{x}_2 + m_2\ddot{\delta} + \gamma k\delta^{\lambda} + \gamma b\delta^{\lambda}\dot{\delta} = 0 \tag{4}$$

According to Newton's second law, Eq. (4) can be rewritten as

$$m_2\ddot{x}_2 = -F(\delta) \tag{5}$$

where

$$F(\delta) = m_2\ddot{\delta} + \gamma k\delta^{\lambda} + \gamma b\delta^{\lambda}\dot{\delta} \tag{6}$$

where $F(\delta)$ is considered a function related to the penetration δ. If the impacted body is not obstructed by other external forces, except for the impacting body, then $F(\delta)$ can be called an interaction force of the cylindrical specimen. Therefore, the interaction force of the impacted body can be described by Eq. (6). However, $F(\delta)$ cannot be defined as the dynamic contact force through the Hunt-Crossley model, which considers the contact force to be a nonlinear spring-dashpot model. The reason is that the term $m_2\ddot{\delta}$ and the coefficient γ in Eq. (6) are not included in the Hunt-Crossley model. Moreover, if the mass of the impacted body equates to the mass of the impacting body, that is, $m_1 = m_2 = m_0$, then the mass coefficient is $\gamma = 1$, and Eq. (6) can be simplified as:

$$F(\delta) = m_0\ddot{\delta} + k\delta^{\lambda} + b\delta^{\lambda}\dot{\delta} \tag{7}$$

III. PIECEWISE NONLINEAR MODEL OF GEAR INTERACTION FORCE

A. NORMAL INTERACTION FORCE COMPONENT

For the gear transmission dynamic analysis under heavy load and low speed, the variation of viscous damping should have a nonlinear relationship to the impact penetration because the output torque of the gear transmission is high in many heavy machinery industries. Moreover, the surface of the tooth may be seriously worn down under heavy load working conditions, and the gear backlash might exist. Therefore, a new normal interaction force equation is established for the driven gear based on Eq. (6) according to the previous description and assuming $\gamma = 1$ as follows:

$$F_n = \begin{cases} m_0\ddot{q} + bg^{\lambda}(q)\dot{q} + kg^{\lambda}(q), & |q| \geq a \\ 0, & |q| < a \end{cases} \tag{8}$$

where k is determined by the material properties and geometrical structure of the contact body, and m_0 is the equivalent mass of the driven gear that can be defined as

$$m_0 = J_2/r_2^2 \tag{9}$$

where J_2 is the total rotary inertia of the driven gear and the load.

In addition, $q = q(t)$ is the dynamic transmission error. Penetration δ can be substituted by transmission error q as $\delta(t) = q(t)$ because the transmission error is commonly considered the impact penetration between the meshing teeth for gear transmission, and q can be expressed as:

$$q = q(t) \approx r_1\theta_1(t) - r_2\theta_2(t) \tag{10}$$

Under the special working conditions with heavy load, the rotary velocity of the gear transmission is very low. For example, the rotary velocity of the heavy-duty forging manipulator investigated in this study ranges from 0-20 rpm. Therefore, meshing stiffness can be considered constant.

Hertzian theory defines meshing stiffness as:

$$k = \tfrac{4}{3}\rho^{\frac{1}{2}}E^* \tag{11}$$

where ρ is the synthetic curvature radius expressed as

$$\frac{1}{\rho} = \frac{1}{\rho_1} + \frac{1}{\rho_2} = \frac{2}{d_1\cos\alpha\tan\alpha'}\frac{u+1}{u}$$

where ρ_1 and ρ_2 are the equivalent curvature radii of gear meshing, which are similar to I_1O and I_2O in Fig. 1, respectively. d_1 is the diameter of the reference circle. α and α' are the pressure angles of the reference and pitch circles, respectively. u is the transmission ratio, and E^* is the comprehensive elastic modulus that is defined as:

$$\frac{1}{E^*} = \frac{1-\upsilon_1^2}{E_1} + \frac{1-\upsilon_2^2}{E_2} \tag{12}$$

where E_1 and E_2 are elastic modules of the two contact bodies, whereas υ_1 and υ_2 are their corresponding Poisson's ratios, respectively. Based on the geometric characteristics of the involute spur gear, the meshing stiffness coefficient becomes

$$k = \frac{4}{3}\left[\frac{ud_1\cos\alpha\tan\alpha'}{2(1+u)}\right]^{\frac{1}{2}} \cdot \left(\frac{1-\upsilon_1^2}{E_1} + \frac{1-\upsilon_2^2}{E_2}\right)^{-1}. \tag{13}$$

$B(q) = bg^n(q)$ is the nonlinear damping model of the dynamic transmission errors obtained by Lankarani *et al.* [36] and is expressed as follows:

$$B(q) = bg^{\lambda}(q) = \frac{3k(1-\tau^2)}{4v}g^{\lambda}(q) \tag{14}$$

where ζ is the restitution coefficient ($0 \leq \zeta \leq 1$) equal to 0.95 N/mm. Table 1 indicates the nonlinear damping model of the dynamic transmission errors based on material property. v is the impact velocity of the contact teeth, which is defined as

$$v = (\omega_1 r_1 - \omega_2 r_2)\cos\alpha \tag{15}$$

The angular velocity of the meshing gear can be determined via simulation or experimental conditions. $g(q)$ is the backlash nonlinear function of gear meshing, which can be expressed as a piecewise function:

$$g(q) = \begin{cases} q-a, q > a \\ 0, -a \leq q \leq a \\ q+a, q < -a \end{cases} \tag{16}$$

where a is the positive value of the half-backlash determined by the geometric dimensioning of the gears and the installation accuracy of meshing gears.

B. TANGENT INTERACTION FORCE COMPONENT

Gear meshing principle posits that the tangential interaction force component of gear transmission be produced by the friction force between the contact teeth. The meshing contact undergoes rolling and sliding processes because of the involute shape of gear teeth, thereby resulting in a sliding friction force that is normal to the line of action. Given the special frequent start-stop working conditions of the heavy-duty forging manipulator, the friction force between the teeth of the heavy-duty gear drive is changed alternatively between the static and dynamic states. Therefore, the bristle model [37], which can describe the difference between dynamic and static friction and can easily be implemented, is introduced to describe the continuous friction contact dynamics. This model can calculate friction force as a function of the vector of bristle displacements and the vector of the normal force F_n. The friction force is defined explicitly and uniquely during the contact at a point. The bristle model that describes the tangent friction force F_t under the special working condition is defined as:

$$F_t = k_f s(t) \tag{17}$$

$$s(t) = \begin{cases} s(t_0) + \int_{t_0}^{t} v_t dt, & |s| < s_{\max} \\ s_{\max} \frac{v_t}{|v_t|}, & otherwise \end{cases} \quad s_{\max} = \mu \frac{|F_n|}{k_f} \tag{18}$$

where k_f is the bristle stiffness, s is the vector of bristle displacement, t_0 is the start time of the last contact point, v_t is the relative tangential velocity related to the rotary velocity of gear meshing, and $s_{\max}$ is the maximum allowable deflection of the bristle based on the material property. Under the lubrication conditions, the sliding friction coefficient of gear meshing is commonly set as $\mu = 0.05$ (Table 1).

C. PIECEWISE NONLINEAR INTERACTION FORCE MODEL

Fig. 4 shows the schematic gear transmission. The total interaction force of the gear transmission can be defined as follows:

$$\vec{F}_c = \sum_{i=1}^{N} \vec{F}_{c,i}, \quad (i = 1 \cdots N) \tag{19}$$

where $\vec{F}_{c,i}$ is the interaction force at each point i between the meshing teeth, and N is the total number of interaction tooth pairs at each meshing time. Based on the analysis in Fig. 4, each interaction force $\vec{F}_{c,i}$ can be decomposed into normal and tangential components and described as:

$$\vec{F}_{c,i} = F_{n,i} \cdot e_{n,i} + F_{t,i} \cdot e_{t,i} \tag{20}$$

where $e_{n,i}$ and $e_{t,i}$ are the normal and tangential unit vectors of the normal and tangential forces, respectively. The gear meshing principle implies that each meshing point is in the common tangent line of the basic circle. Thus, $e_{n,i}$ and $e_{t,i}$ of each meshing point is identical to

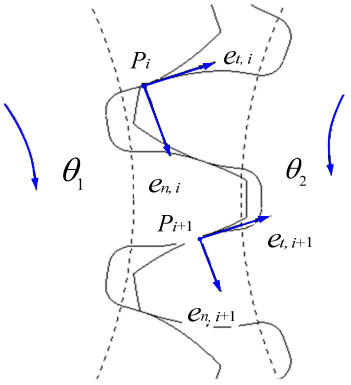

FIGURE 4. Schematic diagram of gear transmission.

$$e_n = e_{n1} = e_{n2} = \cdots = e_{nN}, \quad e_t = e_{t1} = e_{t2} = \cdots = e_{tN} \tag{21}$$

and the relationship of e_n and e_t is

$$\cot \beta = e_t / e_n \tag{22}$$

where β is the meshing angle of gear transmission. Subsequently, Eq. (20) can be rewritten as

$$\vec{F}_{c,i} = F_{n,i} \cdot e_n + F_{t,i} \cdot e_t \tag{23}$$

where scalar $F_{n,i}$ of the normal force is expressed as Eq. (8). Given that the friction during gear meshing is basically a sliding friction, the tangential friction force component can be simplified as

$$F_{t,i} = \mu_i F_{n,i} \tag{24}$$

Combining Eqs. (22)-(24) yields

$$\vec{F}_{c,i} = F_{n,i}(1 + \mu_i \cot \beta) \cdot e_n \tag{25}$$

Substituting Eq. (8) into Eq. (25) yields

$$\begin{aligned} \vec{F}_{c,i}(t) = {} & [m_i \ddot{q}_i(t) + b_i g^{\lambda}(q_i(t)) \dot{q}_i(t) \\ & + k_i g^{\lambda}(q_i(t))](1 + \mu_i \cot \beta) \cdot e_n, (|q_i| \geq a_i) \end{aligned} \tag{26}$$

The parameters of each point at each meshing time are generally considered identical because the meshing teeth of the gear transmission have similar material properties and physical characteristics. In this case, $m_i = \mathbf{M}$, $k_i = \mathbf{K}$, $b_i = \mathbf{B}$, $\mu_i = \mu$ $(i = 1 \cdots N)$. The backlash errors between each of the meshing teeth is extremely small. Thus, the backlash function can also be considered the same approximate function, that is, $a_i = a$, which can be further simplified as $g(q_i) = G_i$. Then, the interaction force of each meshing point

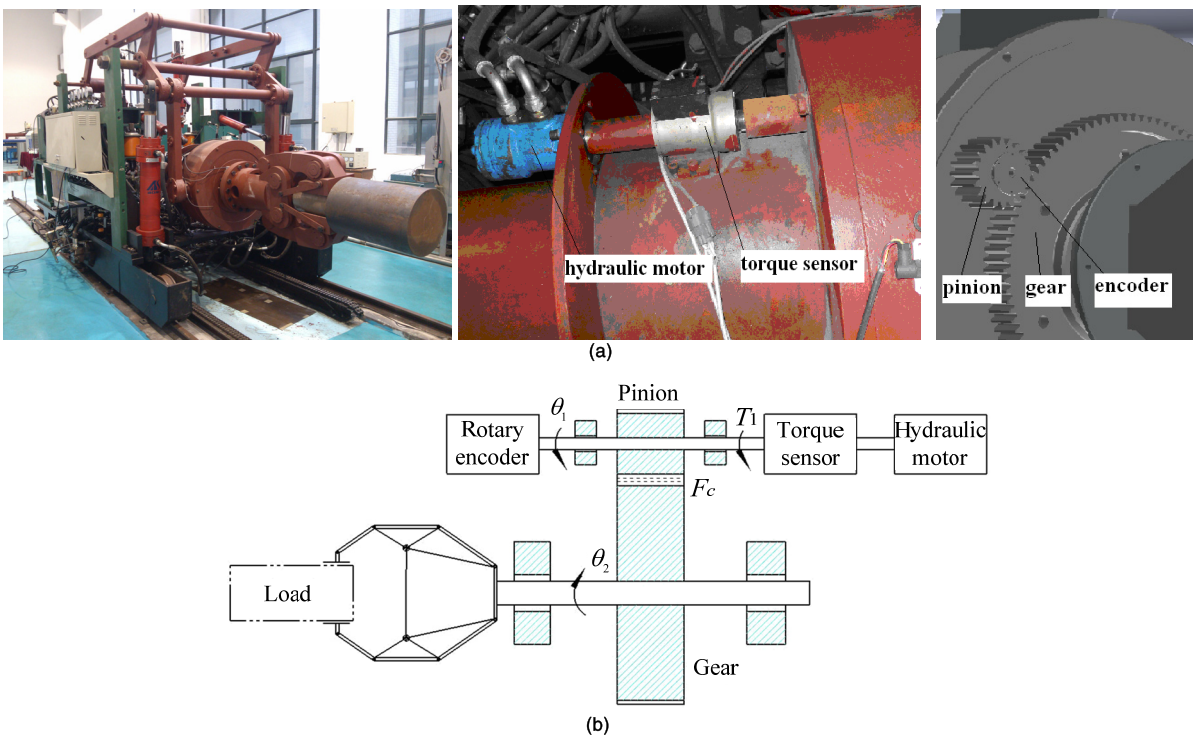

FIGURE 5. Forging manipulator: (a) Experimental set up of the forging manipulator, (b) schematic diagram of gear transmission.

can be rewritten as:

$$\vec{F}_{c,i}(t) = (\mathbf{M}\ddot{q}_i(t) + \mathbf{B}G_i^{\lambda}\dot{q}_i(t) + \mathbf{K}G_i^{\lambda})(1 + \mu\cot\beta)\cdot e_n, \quad (i = 1\cdots N). \tag{27}$$

The scalar form of Eq. (27) can be further obtained as

$$F_{c,i}(t) = (\mathbf{M}\ddot{q}_i + \mathbf{B}G_i^{\lambda}\dot{q}_i + \mathbf{K}G_i^{\lambda})(1+\mu\cot\beta), \quad (i = 1\cdots N). \tag{28}$$

The contact ratio ε of gear transmission is usually between 1 and 2, according to the meshing principle of the gear transmission, that is, $1< \varepsilon <2$. The total interaction force of gear meshing at time t in a meshing period T can be expressed simultaneously as one or more pairs of teeth under alternative meshing state as:

$$\vec{F}_C(t) = \begin{cases} \vec{F}_{c,i-1}(t) + \vec{F}_{c,i}(t) & (\bar{n}-1)T < t \le (1-1/\varepsilon)\,\bar{n}T \\ \vec{F}_{c,i}(t) & (1-1/\varepsilon)\,\bar{n}T < t < (1/\varepsilon)\bar{n}T \\ \vec{F}_{c,i}(t) + \vec{F}_{c,i+1}(t) & (1/\varepsilon)\bar{n}T \le t \le \bar{n}T, \end{cases} \tag{29}$$

where $\vec{F}_C(t)$ is the total interaction force of the gear transmission. $\vec{F}_{c,i-1}$, $\vec{F}_{c,i}$, and $\vec{F}_{c,i+1}$ are the interaction forces at meshing points $i-1$, i, and $i+1$, respectively. $\bar{n}$ is the period serial number ($\bar{n} = 1, 2, 3\ldots$), and T is the full meshing period for a pair of teeth from meshing to separation. Substituting Eq. (28) into Eq. (29), the piecewise nonlinear interaction force model can be obtained as

$$F_C(t) = \begin{cases} [\mathbf{M}(\ddot{q}_{i-1} + \ddot{q}_i) + \mathbf{B}(G_{i-1}^{\lambda}\dot{q}_{i-1} + G_i^{\lambda}\dot{q}_i) \\ \quad +\mathbf{K}(G_{i-1}^{\lambda} + G_i^{\lambda})](1+\mu\cot\beta) \\ \quad (\bar{n}-1) < t \le (1-1/\varepsilon)\,\bar{n}T \\ (\mathbf{M}\ddot{q}_i + \mathbf{B}G_i^{\lambda}\dot{q}_i + \mathbf{K}G_i^{\lambda})(1+\mu\cot\beta) \\ \quad (1-1/\varepsilon)\,\bar{n}T < t < (1/\varepsilon)\bar{n}T \\ [\mathbf{M}(\ddot{q}_i + \ddot{q}_{i+1}) + \mathbf{B}(G_i^{\lambda}\dot{q}_i + G_{i+1}^{\lambda}\dot{q}_{i+1}) \\ \quad +\mathbf{K}(G_i^{\lambda} + G_{i+1}^{\lambda})](1+\mu\cot\beta) \\ \quad (1/\varepsilon)\bar{n}T \le t \le \bar{n}T \end{cases} \tag{30}$$

IV. EXPERIMENTS

The experimental platform is a forging manipulator [6] as shown in the left figure of Fig. 5 (a), which cooperates with a forging press to form forge pieces under heavy load. Fig. 5(b) shows the schematic diagram of the gear transmission. During the forging process, a forge piece that needs to be turned frequently is gripped by a gripper with two tong arms. Therefore, the gear transmission system of the forging manipulator is required to start and stop frequently. The left figure of Fig. 5(a) shows that a forge piece of 290 kg is gripped by the gripper that is driven by the driven gear of the gear transmission system. As shown in the right figure of Fig. 5(a), the pinion drives the driven gear with the gripper to rotate. As shown in the middle figure of Fig. 5 (a), a hydraulic motor controlled by an electrohydraulic proportional valve, a torque sensor and a rotary encoder is

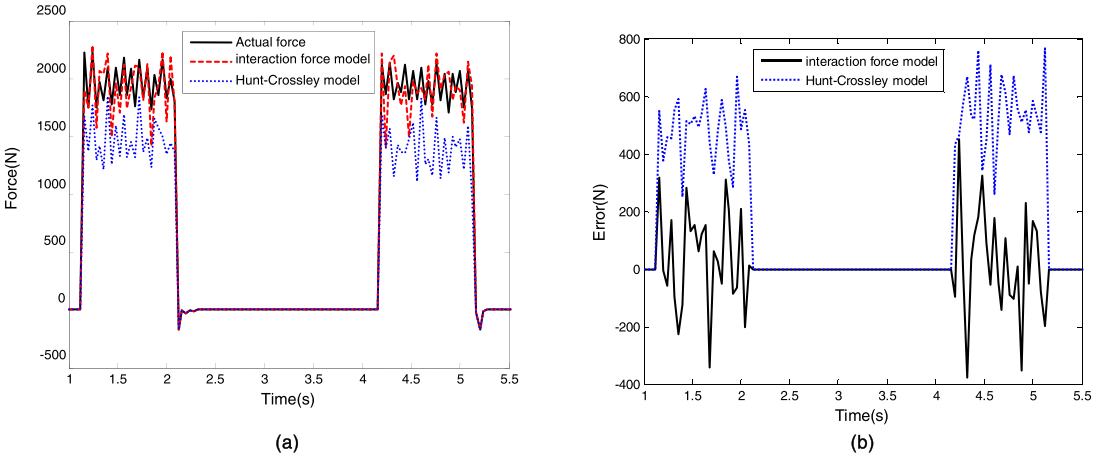

FIGURE 6. Experimental results in start–stop rotation motion: (a) Total interaction force, (b) force errors.

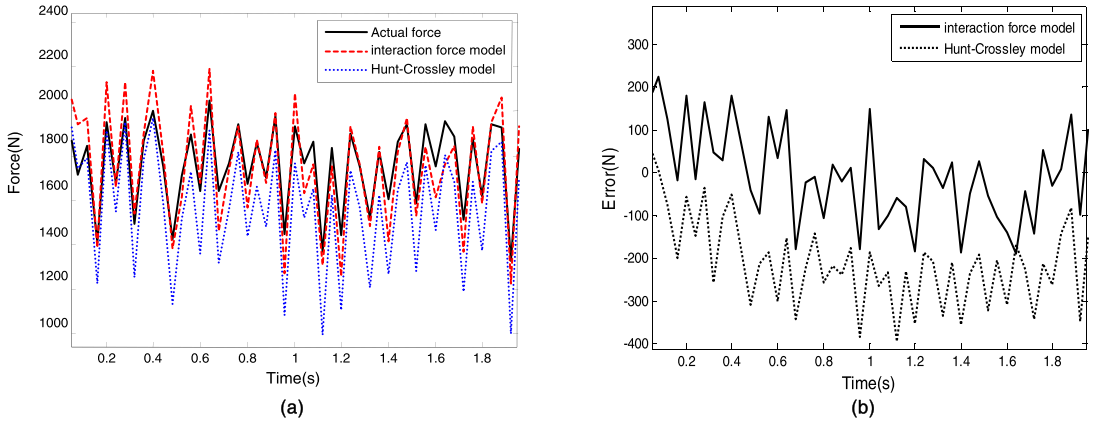

FIGURE 7. Experimental results in continuous rotation motion: (a) Total interaction force, (b) force errors.

installed on the shaft of the driving pinion. The hydraulic motor provides driving torque. The torque sensor is used to measure the output torque of the motor. The rotary encoder can detect the angular displacement, angular velocity and angular acceleration of the pinion. In the experiments, data acquisition and motion control are achieved via SIMOTION D435 (industrial motion control system from SIEMENS, Germany).

Two experiments are carried out. One is the gear transmission experiment with frequent starts and stops. First, a rotary torque of 95 N·m is applied to drive the gripper to rotate. After 1 second, the driving torque is removed, and the rotation stops. The forge piece is forged during the stopping phase for two seconds. Then, the above operation is repeated. Another experiment is the gear transmission experiment under a constant angular velocity, that is, applying a rotary torque of 95 N·m to drive the gripper to rotate continuously. In all the experiments, the gripped forge piece is 290 kg, and the sampling time is 1 ms. The geometrical dimension and physical property parameters of the driving pinion and driven gear are the same as those listed in Table 1.

TABLE 1. Main parameters of gear transmission.

Symbol	Quantity	Value
m	Module	5 mm
r_1, r_2	Radius of gears I_1 and I_2	50 mm, 250 mm
α	Pressure angle	20°
k	Stiffness coefficient	1.72×10^9 N/m
b	Damping coefficient	1.12×10^9 $N{\cdot}s/m$
μ	Friction coefficient	0.05
ζ	Restitution coefficient	0.95 N/mm
ε	Contact ratio	1.749
λ	Power exponent	1.5

The transmission shaft is assumed to be stiff, and the gear meshing is assumed to be perfect. The interaction force in Eq. (30) can be calculated as follows. First, q, $\dot{q}$ and $\ddot{q}$ can be obtained in terms of Eq. (10) with the detected angular displacement, angular velocity and angular acceleration in the experiments. Then, substituting the required parameters, as shown in Table 1, and the calculated q, $\dot{q}$ and $\ddot{q}$ into Eq. (30) yields the calculated interaction force. The practical interaction force of gear transmission in the experiments can be calculated by using $F_c = \tau/r_1$, where the input torque τ is obtained from the torque sensors. Figs. 6 and 7 show the

experimental results of the start-stop and continuous rotating motion conditions, respectively. The collected data are processed and calculated by utilizing data processors, wherein the solid, dashed, and dotted lines denote the interaction forces obtained from the actual collected data, proposed interaction force model, and the Hunt-Crossley model, respectively. The result of the proposed interaction force model is basically consistent with the real experimental result, and the errors in the two different motion conditions are smaller than those of the Hunt-Crossley model. This finding indicates that the proposed interaction force model with the equivalent mass, gear backlash, friction, and contact ratio complements the practical gear transmission characteristics. In addition, Fig. 6a shows that the reverse back impact phenomenon is evident when gear transmission stops. This finding can be explained by the assumption that the driven gear under the interaction of inertia would inversely impact the driving pinion in the stopping phase of gear meshing.

V. CONCLUSION

A piecewise nonlinear dynamic model is proposed for the interaction force of gear transmissions under difficult working conditions. The proposed model combines the equivalent mass, backlash, friction, and contact ratio of gear meshing in the transmission process. The model parameters of the gear transmission can be calculated by using analytical calculation formulas. The experiments are implemented for the gear transmission system of a heavy-duty manipulator under the start-stop rotation and the continuous rotation conditions. The comparative experimental results show that the proposed piecewise nonlinear dynamic model fits the practical mechanical behavior of the gear transmission better than the traditional Hunt-Crossley model. This finding indicates that the application of the proposed model in the nonlinear dynamic analysis of gear transmissions under difficult working conditions is suitable. In our future work, the proposed model will be used to design an optimal control system that requires an analytic model to accurately describe the dynamic behavior of gear transmissions.

REFERENCES

[1] S. A. Abhari, F. Hashemzadeh, M. Baradarannia, and H. Kharrati, "An adaptive robust control scheme for robot manipulators with unknown backlash nonlinearity in gears," *Trans. Inst. Meas. Control*, vol. 41, no. 10, pp. 2789–2802, Jun. 2019.
[2] X. Lei and J. Wang, "Dynamic analysis of the vehicle-track coupling system with finite elements in a moving frame of reference," *J. Vib. Control*, vol. 20, no. 9, pp. 1301–1317, 2014.
[3] F. van der Linden and L. J. Franciscus, "Modeling of geared positioning systems: An object-oriented gear contact model with validation," *Proc. Inst. Mech. Eng., C, J. Mech. Eng. Sci.*, vol. 230, nos. 7–8, pp. 1084–1100, Apr./May 2016.
[4] H. Yazici and M. Sever, "Active control of a non-linear landing gear system having oleo pneumatic shock absorber using robust linear quadratic regulator approach," *Proc. Inst. Mech. Eng., G, J. Aerosp. Eng.*, vol. 232, no. 13, pp. 2397–2411, Oct. 2018.
[5] X.-H. Liang, H.-S. Zhang, M.-J. Zuo, and Y. Qin, "Three new models for evaluation of standard involute spur gear mesh stiffness," *Mech. Syst. Signal Process.*, vol. 101, pp. 424–434, Feb. 2018.
[6] Z. Xu, "Dynamic modeling of parallel driving and load balance control for the gripping system of heavy-duty forging manipulators," Ph.D. dissertation, School Mech. Elect. Eng., Central South Univ., Changsha, China, 2013.
[7] J. Yoon, J. Kim, J. Seo, and S. Suh, "Spatial factors affecting the loading efficiency of excavators," *Automat. Construct.*, vol. 48, pp. 97–106, Dec. 2014.
[8] N. Luan, H. Zhang, and S. Tong, "Optimum motion control of palletizing robots based on iterative learning," *Ind. Robot, Int. J.*, vol. 39, no. 2, pp. 162–168, 2012.
[9] W.-H. Ding, H. Deng, Q.-M. Li, and Y.-M. Xia, "Control-orientated dynamic modeling of forging manipulators with multi-closed kinematic chains," *Robot. Comput. Integr. Manuf.*, vol. 30, no. 5, pp. 421–431, Oct. 2014.
[10] G. P. Prajapat, N. Senroy, and I. N. Kar, "Modeling and impact of gear train backlash on performance of DFIG wind turbine system," *Electr. Power Syst. Res.*, vol. 163, pp. 356–364, Oct. 2018.
[11] P. Ziegler and P. Eberhard, "Simulative and experimental investigation of impacts on gear wheels," *Comput. Method. Appl. Mech. Eng.*, vol. 197, nos. 51–52, pp. 4653–4662, 2008.
[12] Y. Guo, S. Lambert, R. Wallen, R. Errichello, and J. Keller, "Theoretical and experimental study on gear-coupling contact and loads considering misalignment, torque, and friction influences," *Mech. Mach. Theory*, vol. 98, pp. 242–262, Apr. 2016.
[13] S. He, R. Gunda, and R. Singh, "Effect of sliding friction on the dynamics of spur gear pair with realistic time-varying stiffness," *J. Sound Vib.*, vol. 301, nos. 3–5, pp. 927–949, Apr. 2007.
[14] L. Han, L. Xu, and H. Qi, "Influences of friction and mesh misalignment on time-varying mesh stiffness of helical gears," *J. Mech. Sci. Technol.*, vol. 31, no. 7, pp. 3121–3130, Jul. 2017.
[15] S. He, S. Cho, and R. Singh, "Prediction of dynamic friction forces in spur gears using alternate sliding friction formulations," *J. Sound Vib.*, vol. 309, nos. 3–5, pp. 843–851, Jan. 2008.
[16] H. Dong, Z.-Y. Liu, L.-L. Duan, and Y.-H. Hu, "Research on the sliding friction associated spur-face gear meshing efficiency based on the loaded tooth contact analysis," *PLoS One*, vol. 13, no. 6, Jun. 2018, Art. no. e0198677, doi: 10.1371/journal.pone.0198677.
[17] S.-S. Ge, D.-T. Qin, M.-H. Hu, and Y.-G. Liu, "Active torque control for gear dynamic load suppression in a drum shearer cutting transmission system under impact loads," *J. Sound Vib.*, vol. 24, no. 21, pp. 5072–5086, Nov. 2018.
[18] S. Li and A. Anisetti, "A tribo-dynamic contact fatigue model for spur gear pairs," *Int. J. Fatigue*, vol. 98, pp. 81–91, May 2017.
[19] Y. Gao, B. Chen, R. Tan, and Y. Zhang, "Design and finite element analysis for helical gears with pinion circular arc teeth and gear parabolic curve teeth," *J. Adv. Mech. Des. Syst. Manuf.*, vol. 10, no. 1, 2016, Art. no. JAMDSM0009.
[20] T. Lin, H. Ou, and R. Li, "A finite element method for 3D static and dynamic contact/impact analysis of gear drives," *Comput. Methods Appl. Mech. Eng.*, vol. 196, nos. 9–12, pp. 1716–1728, 2007.
[21] J.-R. Cho, K.-Y. Jeong, M.-H. Park, D.-S. Shin, O.-K. Lim, and N.-G. Park, "Finite element structural analysis of wind turbine gearbox considering tooth contact of internal gear system," *J. Mech. Sci. Technol.*, vol. 27, no. 7, pp. 2053–2059, Jul. 2013.
[22] Z. Xu, H. Deng, and Q. Wang, "Modeling of multiteeth contact meshing gear dynamics with backlash and coincidence degree," *Adv. Mater. Res.*, vols. 562–564, pp. 842–846, Aug. 2012.
[23] W.-N. Yu and C. K. Mechefske, "Analytical modeling of spur gear corner contact effects," *Mech. Mach. Theory*, vol. 96, pp. 146–164, Feb. 2016.
[24] E. Sakaridis, V. Spitas, and C. Spitas, "Non-linear modeling of gear drive dynamics incorporating intermittent tooth contact analysis and tooth eigenvibrations," *Mech. Mach. Theory*, vol. 136, pp. 307–333, Jun. 2019.
[25] M. Cirelli, P. P. Valentini, and E. Pennestrì, "A study of the non-linear dynamic response of spur gear using a multibody contact based model with flexible teeth," *J. Sound Vib.*, vol. 445, pp. 148–167, Apr. 2019.
[26] W. Mo, Y. Jiao, and Z. Chen, "Dynamic analysis of helical gears with sliding friction and gear errors," *IEEE Access*, vol. 6, pp. 60467–60477, 2018.
[27] G. Gilardi and I. Sharf, "Literature survey of contact dynamics modelling," *Mech. Mach. Theory*, vol. 37, no. 10, pp. 1213–1239, Oct. 2002.
[28] M. Weber, K. Patel, O. Ma, and I. Sharf, "Identification of contact dynamics model parameters from constrained robotic operations," *J. Dyn. Syst. Meas. Control*, vol. 128, no. 2, pp. 307–318, Jun. 2006.
[29] S. Bajpai, N. Nataraj, and A. K. Pani, "On a two-grid finite element scheme for the equations of motion arising in Kelvin–Voigt model," *Adv. Comput. Math.*, vol. 40, nos. 5–6, pp. 1043–1071, Dec. 2014.
[30] I. Pavlović, R. Pavlović, I. Ćirić, and D. Karličić, "Dynamic stability of nonlocal Voigt–Kelvin viscoelastic Rayleigh beams," *Appl. Math. Model.*, vol. 39, no. 22, pp. 6941–6950, Nov. 2015.

[31] A. Haddadi and K. Hashtrudi-Zaad, "Real-time identification of hunt–crossley dynamic models of contact environments," *IEEE Trans. Robot.*, vol. 28, no. 3, pp. 555–566, Jun. 2012.
[32] K. Hunt and F. Crossley, "Coefficient of restitution interpreted as damping in vibroimpact," *J. Appl. Mech.*, vol. 42, no. 2, pp. 440–445, Jun. 1975.
[33] D. Erickson, M. Weber, and I. Sharf, "Contact stiffness and damping estimation for robotic systems," *Int. J. Robot. Res.*, vol. 22, no. 1, pp. 41–57, Jan. 2003.
[34] Y. Zhang and I. Sharf, "Force reconstruction for low velocity impacts using force and acceleration measurements," *J. Vib. Control*, vol. 17, no. 3, pp. 407–420, May 2011.
[35] M. B. Sánchez, M. Pleguezuelos, and J. I. Pedrero, "Approximate equations for the meshing stiffness and the load sharing ratio of spur gears including hertzian effects," *Mech. Mach. Theory*, vol. 109, pp. 231–249, Mar. 2017.
[36] H. M. Lankarani and P. E. Nikravesh, "A contact force model with hysteresis damping for impact analysis of multibody systems," *J. Mech. Des.*, vol. 112, no. 3, pp. 369–376, 1990.
[37] J. Liang, S. Fillmore, and O. Ma, "An extended bristle friction force model with experimental validation," *Mech. Mach. Theory*, vol. 56, pp. 123–137, Oct. 2012.

ZHEN XU received the B.S. degree in mechanical and electrical engineering from the Henan University of Science and Technology, Luoyang, Henan, in 2005, and the Ph.D. degrees in mechanical engineering from the Central South University, Changsha, Hunan, in 2013. Since 2013, he has been engaged in intelligent control of shield machine in the China Railway Construction Heavy Industry Company, Ltd. His current research interests are complexity system modeling, intelligent control, neural network internal model control, and construction robot design.

HUA DENG (M'12) received the B.E. degree in electrical engineering from the Nanjing Aeronautical Institute, Nanjing, China, in 1983, the M.E. degree in electrical engineering from Northwestern Polytechnical University, Xi'an, China, in 1988, and the Ph.D. degree in manufacturing engineering from the City University of Hong Kong, Hong Kong, in 2005. He is currently a Professor with the School of Mechanical and Electrical Engineering, Central South University, Changsha, China. His research interests include intelligent control and learning, robotic dynamics and control, biomechatronics, and modeling and control of complex distributed parameter systems.

YI ZHANG received the B.E. and Ph.D. degrees from the School of Mechanical and Electrical Engineering, Central South University, China. He is currently a Postdoctoral Fellow with the School of Mechanical and Electrical Engineering, Central South University. He is also a Lecturer with the School of Mechanical and Electrical Engineering, Changsha University, China. His current research interests include mechanism design, and system modeling and control.